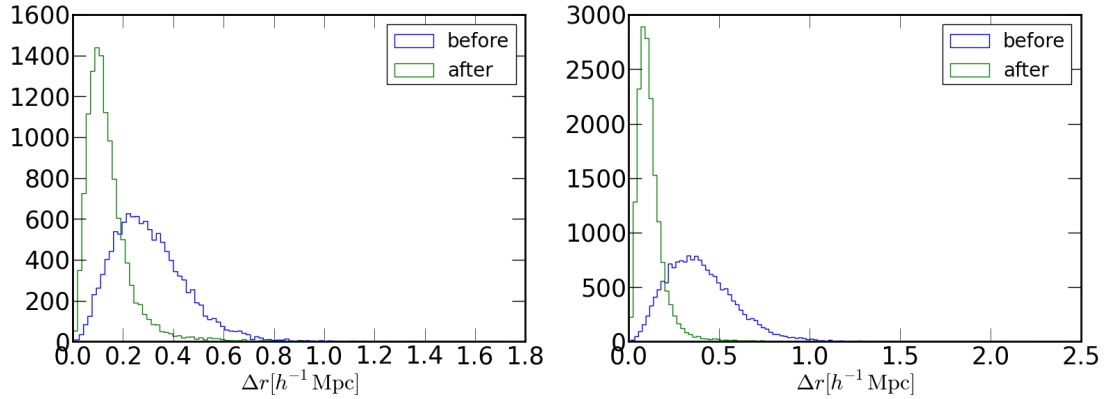

Fig. 1: Histograms of distance for the matched halos at $z = 0.8$ and $z = 0.7$ (left) and at $z = 0.25$ and $z = 0.15$ (right). The blue line represents the distribution of the distance before shifting and the green line is after shifting. Both plots show that the distances between the halos at different redshifts become smaller after the shifting.

1 Light cone

In this section, we describe how we construct a light cone output from the simulation. We have outputs at fixed redshift from $z = 0.8$ to $z = 0.15$ for every 0.1. We first put an observer at the center of the simulation box, and cut out each output to a spherical shell whose radius corresponds to the redshift of the output. Then, we assemble the spherical shells consecutively. At this point, a corresponding redshift of each object in the light cone output is the redshift of the spherical shell where the object belongs to. In other words, the redshift distribution in the light cone output is discrete. The observational universe, however, has a smooth distribution of redshift, since redshift corresponds to the radial distance of each object. In order to recover the smooth correspondence between redshift and radial distance from the observer, we shift the position of each object from the redshift of the output z_{sim} to its positional redshift z_{pos} with its velocity.

1.1 Consistency Check

Here, we show some tests we ran to make sure that shifting the position of halos do not alter any physics and the nature of halo distribution. For the comparison, we choose two redshifts z_1 and z_2, and shift the halos in one sample at $z = z_1$ to $z = z_2$. We compare the distances for the halos which exist at both redshifts. Figure 1 is the histograms of positional differences at $z = 0.8$ and $z = 0.7$ and also at $z = 0.25$ and $z = 0.15$ before and after shifting. We pick up high and low redshifts to show that our results are redshift independent. After shifting halos, we see that the mean distance between corresponding halos becomes closer and the scatter decreases, as shown in Table 1.

Second, we evaluate how the distribution of halos is changed after shifting by computing power spectra. Figure 2 shows the cross power spectra between DM particles and halos before and after shifting. Those cross power spectra agree well up to 1 $h\mathrm{Mpc}^{-1}$. Both Figure 1 and 2 show that shifting halos do not alter any statistical property that original halo distribution possesses.

from $z = 0.8$ to $z = 0.7$	mean $[h^{-1}\mathrm{Mpc}]$	std $[h^{-1}\mathrm{Mpc}]$
before	0.306	0.152
after	0.143	0.105
from $z = 0.25$ to $z = 0.15$	mean $[h^{-1}\mathrm{Mpc}]$	std $[h^{-1}\mathrm{Mpc}]$
before	0.399	0.192
after	0.123	0.097

Tab. 1: Mean separation and the standard deviations of the halos at different redshifts before and after shifting.

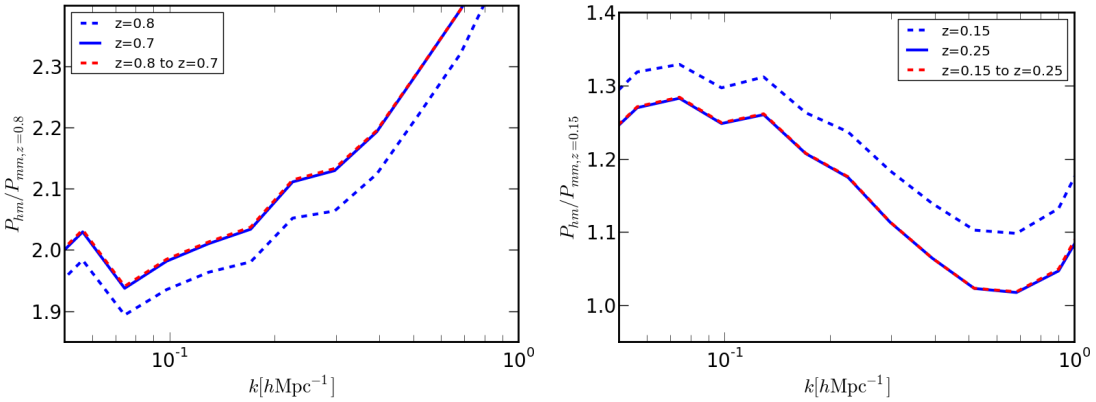

Fig. 2: Ratio of halo-matter cross power spectra with respect to matter auto power spectra at $z = 0.8$ (left) and $z = 0.15$ (right) respectively. In the left panel, we compare the original power spectra at $z = 0.8$ (blue dashed line) and $z = 0.7$ (blue line) to the power spectra for the halos shifted from $z = 0.8$ to $z = 0.7$ (red dashed line). The right panel has the same format as the left, but we shift the halos from $z = 0.15$ to $z = 0.25$. Both plots show that the power spectra after shifting agree well with the power spectra at the redshift of destination and preserves the statistical property.

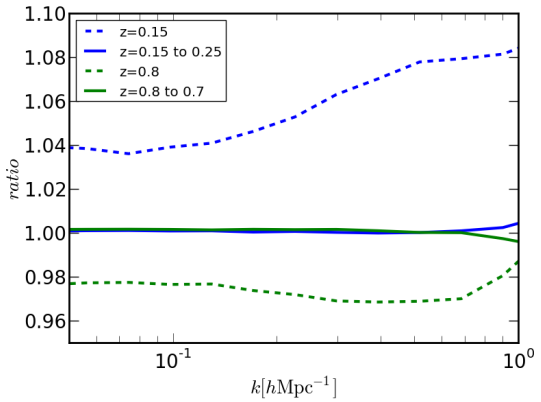

Fig. 3: This is the alternative plot for Figure 2

2 THE BOSS SIMULATIONS

- Simulation Parameters: Nikhil

describe box size, masses, geometry etc. Show that we can fit in two BOSS volumes per box. Also, mention that we decide to use the 300/2 simulations (as an example here).

2.1 Building the Galaxy Catalog

To generate galaxy mock catalogs, we need to go through the following steps:

1) populate halos with galaxies through the HOD functional form,

2) give positions and velocities to the galaxies assuming an NFW profile (Navarro, Frenk & White 1996).

The HOD functional form gives probabilities for the number of central and satellite galaxies based on mass of halos which host those galaxies with five free parameters. For each halo, the number of central galaxies is either 0 or 1 given by $N_{cen}(M)$, and the number of satellite galaxies is given by Poisson distribution with a mean $N_{sat}(M)$:

$$N_{cen}(M) = \frac{1}{2}\mathrm{erfc}\left[\frac{\ln(M_{cut}/M)}{\sqrt{2}\sigma}\right], \tag{1}$$

and

$$N_{sat}(M) = N_{cen}(M)\left(\frac{M-\kappa M_{cut}}{M_1}\right)^{\alpha}, \tag{2}$$

where M_{cut}, M_1, σ, κ, and α are free parameters and M is a halo mass. Note that $N_{sat}(M)$ is zero when $M < \kappa M_{cut}$. Note that halos do not host satellite galaxies without a central galaxy. The total number of galaxies hosted by each halo is a sum of the number of central and satellite galaxies. There are several different functional forms used in different papers, but there is little difference on distribution of central and satellite galaxies between those different functionals.

Now, we need to give positions and velocities to those populated galaxies. For central galaxies, their positions are always at the center of the halos and their velocities are the same as the velocities of the halos hosting those central galaxies. For satellite galaxies, we place them randomly assuming the NFW profile:

$$\rho(r) = \frac{4\rho_s}{\frac{r}{r_s}(1+\frac{r}{r_s})}, \tag{3}$$

where r_s is the characteristic radius defined as $r_s = R_{vir}/c$, where R_{vir} is a virial radius for a halo and c is the concentration parameter. The distance r from the center of the halo is given by the probability based on the NFW profile. There have been several studies how to describe the concentration parameter c as a function of halo mass and redshift (citations). In this paper, we used the formula presented in Klypin et al. 2010:

$$c(M,z) = \frac{c_0}{1+z}(M-M_0)^{-\beta}, \tag{4}$$

where$c_0 = 9.60$, $M_0 = 10^{12\cdot}$, and $\beta = 0.75$.

We assign velocities to the satellite galaxies by using the virial theorem. The virial theorem states that the mean kinetic energy of the system is equivalent to half the mean potential energy, as shown below:

$$< v^2 >= \frac{GM}{R_{vir}}. \tag{5}$$

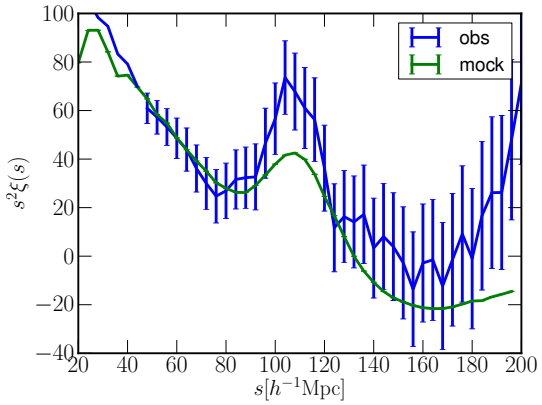

Fig. 4: Correlation function monopoles $\xi(s)$ of the mocks (green) and of the CMASS galaxy measured in **?** (blue) at $z = 0.55$. The BAO peak of the mock correlation function is smoothed due to the wide window function.

We draw a Gaussian distribution with zero mean and variance in Eq. 5 to give an internal velocity for the satellite galaxies. Here, we assume that satellite galaxies are randomly moving inside the host halos. So, we give the radial component of this random motion from the Gaussian distribution and determine the direction randomly with equal probability. Note that the total velocity of the satellite galaxies is given as the sum of the halo velocity at the center of the host halo and the velocity contributed as a random motion inside the halo.

Now, we generate galaxy mocks with our samples at $z = 0.55$. In Figure 4, we compare the correlations function $\xi(s)$ with the one in Anderson et al. (2013), where s is the redshift-space coordinate. Here, we use the following HOD parameters:

$M_{cut} = 12.9$,
$M_1 = 14.05$,
$\alpha = 0.9$,
$\kappa = 1.13$,
$\sigma = 0.74$.

Note that we compute the correlation functions in the redshift-space with periodic boundary condition (If we decide to use the correlation function computed after cutting out and fitting to n(z), I need to change this part). The correlation function computed from our sample mocks fits to the correlation function in Anderson et al. 2013 well on the scale between $30h^{-1}$Mpc and $80h^{-1}$Mpc. Due to the large smoothing scale (i.e., the grid size used to compute $\xi(s)$ is about $8h^{-1}$Mpc), our BAO peak is more smoothed out than the one in Anderson et al. 2013.